Systems/Circuits

Role of Inhibition in Respiratory Pattern Generation

Wiktor A. Janczewski,[1] **Alexis Tashima,**[1] **Paul Hsu,**[1] **Yan Cui,**[1,2] **and Jack L. Feldman**[1]

[1]Department of Neurobiology, David Geffen School of Medicine, University of California, Los Angeles, Los Angeles, California 90095-1763, and [2]Department of Physiology, West China School of Preclinical and Forensic Medicine, Sichuan University, Chengdu, Sichuan 610041, People's Republic of China

Postsynaptic inhibition is a key element of neural circuits underlying behavior, with 20 –50% of all mammalian (nongranule) neurons considered inhibitory. For rhythmic movements in mammals, e.g., walking, swimming, suckling, chewing, and breathing, inhibition is often hypothesized to play an essential rhythmogenic role. Here we study the role of fast synaptic inhibitory neurotransmission in the generation of breathing pattern by blocking $GABA_A$ and glycine receptors in the preBötzinger complex (preBötC), a site essential for generation of normal breathing pattern, and in the neighboring Bötzinger complex (BötC). The breathing rhythm continued following this blockade, but the lung inflation-induced Breuer–Hering inspiratory inhibitory reflex was suppressed. The antagonists were efficacious, as this blockade abolished the profound effects of the exogenously applied $GABA_A$ receptor agonist muscimol or glycine, either of which under control conditions stopped breathing in vagus-intact or vagotomized, anesthetized, spontaneously breathing adult rats. In vagotomized rats, $GABA_A$ergic and glycinergic antagonists had little, if any, effect on rhythm. The effect in vagus-intact rats was to slow the rhythm to a pace equivalent to that seen after suppression of the aforementioned Breuer–Hering inflation reflex. We conclude that postsynaptic inhibition within the preBötC and BötC is not essential for generation of normal respiratory rhythm in intact mammals. We suggest the primary role of inhibition is in shaping the pattern of respiratory motor output, assuring its stability, and in mediating reflex or volitional apnea, but not in the generation of rhythm per se.

Introduction

Rhythmic movements in mammals, e.g., walking, swimming, suckling, chewing, and breathing, involve alternating activation of antagonistic muscles: flexors/extensors, inspiratory/expiratory, abductors/adductors. One longstanding hypothesis is that these rhythms are generated by mutually inhibitory groups of neurons [e.g., "half-centers" in the study by Brown (1914)]. Such reciprocal inhibition provides a straightforward explanation of why one phase of rhythm is silent while the other is active. This idea was adopted for breathing in an inspiratory– expiratory "half center" model (Burns, 1963), which was subsequently refined into an "off-switch" hypothesis, where high-threshold inhibitory neurons terminated the inspiratory phase (Rubio, 1972; Bradley et al., 1975; and Feldman and Cowan, 1975; Younes et al., 1978; von Euler, 1983). Subsequently, reciprocal inhibition between early inspiratory neurons and postinspiratory (post-I) neurons was postulated as the rhythmogenic mechanism (Richter, 1982; Richter et al., 1992). These models were hampered by lack of clear

identification of brainstem structures and associated neurons critical for rhythmogenesis. The identification of the Bötzinger complex (BötC) (Kalia et al., 1979) and demonstration that it contained several populations of inhibitory neurons, including postinspiratory and augmenting expiratory (Fedorko and Merrill, 1984; Ezure et al., 2003a,b; Smith et al., 2007), and of the preBötzinger complex (preBötC) (Feldman et al., 1990; Smith et al., 1991), which contains excitatory neurons critical for normal breathing in intact mammals (Tan et al., 2008) as well as a substantial population of inhibitory neurons (Winter et al., 2009), provided a basis for further refinement of models where inhibition was critical for rhythmogenesis. In a current model of this type, an inhibitory "ring" of early inspiratory neurons in the preBötC and postinspiratory neurons and augmenting expiratory neurons in the BötC (Smith et al., 2007, their Fig. 8A) is proposed to generate normal respiratory rhythm in intact mammals (Smith et al., 2007, 2012). This model predicts that blockade of inhibition at its proposed sites of action the preBötC and BötC should produce apnea (Smith et al., 2007, their Figs. 12, 13C).

To evaluate the role of fast synaptic (GABA_A- and glycine-mediated) inhibition in generation of respiratory pattern, we injected effective antagonists into both the preBötC and BötC in anesthetized, spontaneously breathing adult rats. In vagotomized rats, breathing frequency did not change. In vagus-intact rats, frequency slowed to that of vagotomized rats, while the Breuer–Hering inspiratory inhibitory inflation reflex was suppressed. A complementary strategy to suppress inhibition was to ablate a critical source in the BötC, with the result that a normal breathing pattern continued. We conclude that postsynaptic inhibition within the preBötC and BötC is not essential for generation of
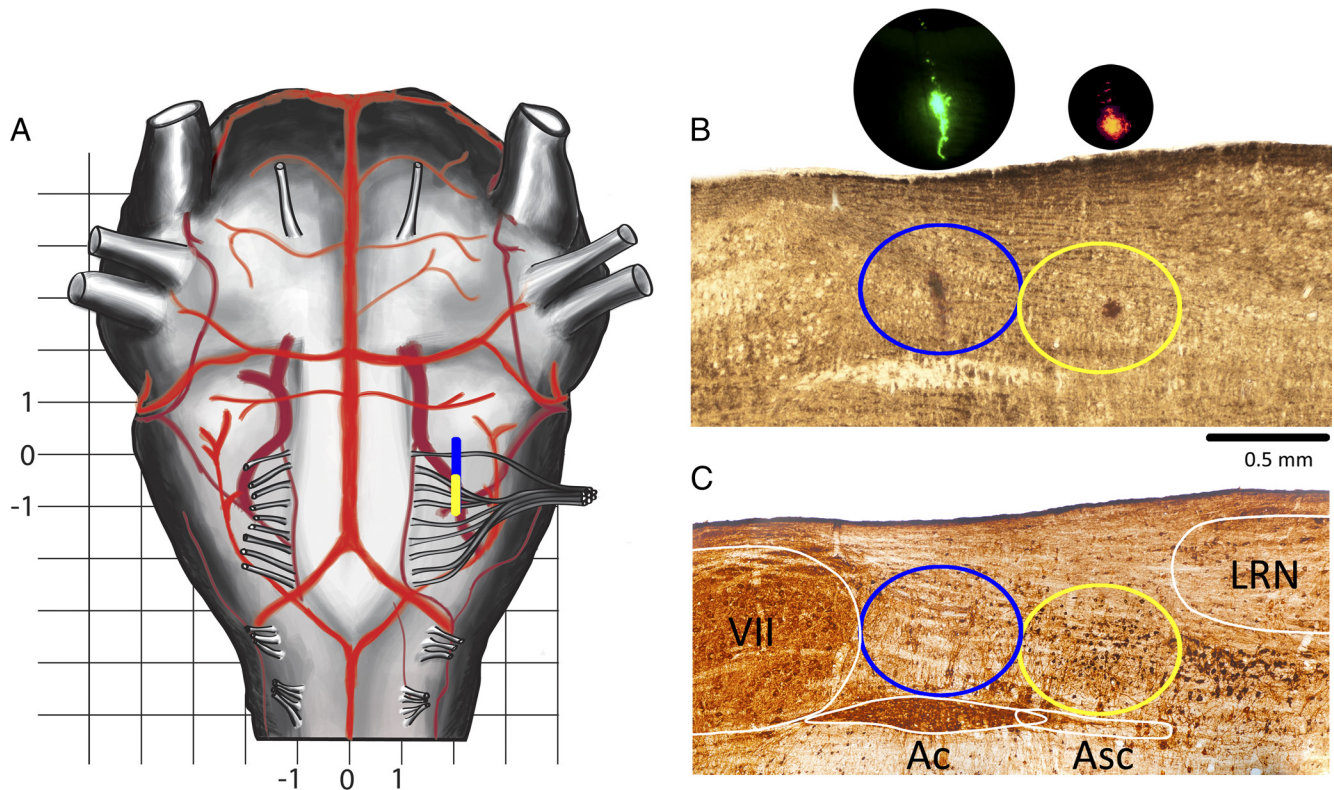
Figure 1. Histology. *A*, Schema of ventral brainstem surface. Rostrocaudal extension of the preBötC/BötC is marked by a yellow/blue bar. Grid scale, 1 mm. Zero in the rostrocaudal direction is at the level of the most rostral root of XIIn. *B*, Sagittal section 2 mm lateral to midline; fresh wet tissue before processing. Yellow/blue ellipses encompass the preBötC/BötC. In bright field, FluoSpheres are visible as a darkened area; inserts are in dark field (DAPI filter cube). *C*, Nickel-enhanced reelin (brown-black) plus ChAT (light brown) double-DAB staining. Note the small (~16 μm) neurons in the preBötC and larger (~26 μm) neurons just caudal to the preBötC (Tan et al., 2012). The slice in *C* was rescaled (1.15× rostrocaudally and 1.2× dorsoventrally) to compensate for shrinkage. Yellow/blue ellipses encompass the preBötC/BötC. VII, Facial motor nucleus.

normal respiratory rhythm in intact mammals. We suggest that the principal roles of inhibition essential for regulation of ventilation in real-world conditions in intact mammals are nonrhythmogenic and include modulation of frequency, shaping of respiratory motor output pattern and assuring its stability, control of upper airway resistance, gating of active expiration, and mediating reflex or volitional apnea.

Materials and Methods

General procedures and injections. Experimental protocols were approved by the University of California, Los Angeles, Animal Research Committee. Male Sprague Dawley rats (Charles River Farms), weighing 320–470 g, were anesthetized with ketamine and xylazine (100 and 10 mg/kg, respectively, i.p.). Atropine (0.5 mg/kg, i.p.) was given to prevent bradycardia and excessive airway secretion. Isoflurane (1–2% vol in air) was administered throughout an experiment. The level of anesthesia was assessed by the suppression of the withdrawal reflex and by the absence of changes in heart rate and breathing rate in response to noxious stimuli. The rats were placed in a supine position in a stereotaxic instrument (David Kopf Instruments). The larynx was denervated, separated from the pharynx, and moved aside. A tracheostomy tube was placed in the trachea through the larynx; under these conditions, spontaneous breathing was unaffected by upper airway afferents. The basal aspect of the occipital bone was removed to expose the ventral aspect of the medulla.

Location of the preBötC and BötC. The preBötC and BötC have fixed positions in relation to the nucleus ambiguous subcompact (Asc) and compact (Ac), caudal pole of the facial nucleus (cVII), and lateral reticular nucleus (LRN), as established by studies using specific markers for preBötC neurons (Gray et al., 1999; Tan et al., 2012). On a parasagittal section through the preBötC as presented in Figure 1, *B* and *C*, the rostrocaudal extent of the preBötC plus BötC (preBötC+BötC) is ~1.3 mm,

in between the cVII [corresponding to 11.85 mm caudal to bregma in the work of Paxinos et al. (1999, their Fig. 146)] and the LRN [corresponding to 13.1 mm caudal to bregma in the work of Paxinos et al. (1999, their Fig. 177)]. The BötC is ventral to Ac, and the preBötC is ventral to Asc with the center of BötC/preBötC approximately aligned with the center of Ac/Asc (Gray et al., 1999, their Fig. 2; Smith et al., 2007, their Figs. 1, 2; Tan et al., 2010, their Fig. 9; Tan et al., 2012, their Fig. 3).

A ventral approach to the medulla is advantageous to target the preBötC+BötC due to their proximity and their position relative to easily visible protuberances of the ventral medullary surface associated with the facial nucleus and various cranial nerve roots. The most rostral root of the hypoglossal nerve (RRXII) is unique because it is thinner and separated from other roots, and thus suitable as a landmark. The entry point of the RRXII [12 mm caudal to bregma in a 274 g Wistar male rat in the work of Paxinos et al. (1999, their Fig. 150)] is at the same rostrocaudal level as the rostral half of the BötC. Injections targeted to the center of the BötC were made 50 μm caudal to the RRXII, i.e., 300 μm caudal to the cVII, 2.1 mm lateral to the midline, and 600 μm dorsal to the ventral medullary surface. Injections targeted to the center of the preBötC were placed 750 μm caudal from the RRXII, i.e., 1000 μm caudal to the cVII (Fig. 1), 2 mm lateral to the midline, and 700 μm dorsal to the ventral medullary surface. Small corrections were made to avoid puncturing of blood vessels on the surface of the medulla. Fluorescent polystyrene beads (2–5% vol) were added to the injectate for *post hoc* confirmation of injection sites. We used three types of 0.2 μm FluoSpheres (Invitrogen): Orange (catalog # F8809), Yellow-Green (catalog #F8764), and Red (catalog #F8763). Under fluorescent illumination with DAPI filtering, they appear yellow, green, and red, respectively.

Experimental groups. Data were obtained from 39 anesthetized adult rats (320–470 g) divided into seven groups. Group 1 (*n* = 5) and Group 2 (*n* = 5) tested the effectiveness of using bicuculline (B) and strychnine

(S) in blocking synaptic inhibition in vagotomized rats (Figs. 2, 3; Table 1). Group 3 ($n = 6$) determined the disturbances of breathing resulting from bilateral injection of vehicle alone (110 μl of saline saline) into the preBötC and BötC. Group 4 ($n = 7$) tested the effects of injecting a mixture of bicuculline and strychnine (B+S) into the preBötC and BötC on breathing pattern in adult anesthetized spontaneously breathing rats with intact vagi. Group 5 ($n = 6$) was similar to Group 4, except that rats were vagotomized (see Fig. 6; Table 2). Group 6 ($n = 5$) tested the effects of B+S injections on recurrent laryngeal nerve (RLN) activity, which has a postinspiratory component. Group 7 ($n = 5$) tested the effect of ablation of the BötC, the region containing post-I and augmenting expiratory (aug-E) inhibitory neurons, on breathing pattern (see Fig. 8; Table 2).

Agonist–antagonist–agonist injections (Groups 1 and 2). Bicuculline [prepared from bicuculline methiodide powder; molecular weight (MW), 509.3; catalog #2503, Tocris Bioscience] was used to antagonize $GABA_A$ receptors, and strychnine (prepared from strychnine HCl powder; MW, 370.9; catalog #S8753, Sigma-Aldrich) was used to antagonize glycine receptors. In preliminary studies, we determined that the lowest concentration of agonist that resulted in prolonged (>4 min) apnea in every rat was 95 μM muscimol, ~90 nl per side, or 5.7 mM glycine (110 nl) injected into the preBötC. The concentration of B+S (238 μM each) was chosen so that that there was no change in breathing when an agonist was injected after B+S. Our concentration of glycine (5.7 mM) was almost the same as used to produce apnea (6 mM) by Chitravanshi and Sapru (2002). Muscimol (300 μM) was used to trigger apnea in the study by Bongianni et al. (2010). Various concentrations of B+S blocked inhibition in previous studies. Pierrefiche et al. (1998) used 100 μM of B+S. Bongianni et al. (2010) used 5 mM bicuculline and 5 mM strychnine. To confirm the efficiency of B+S injections in blocking receptors, muscimol (MW, 114.1; catalog #M1523, Sigma-Aldrich) or glycine (MW, 75.1; catalog #S8753, Sigma-Aldrich) was injected bilaterally into the preBötC; this resulted in apnea. B+S were then injected into the same place to restore the rhythm, and then muscimol or glycine were injected again. Agonist–antagonist–agonist injections were placed in the same spot, as verified by overlap of three different colors of FluoSpheres, one for each solution (Fig. 2D). The ventral approach facilitated multiple injections into the same spot because the entry point of a previous injection was visible in dark field under our surgical microscope.

Saline control injections (Group 3). In Group 3, instead of injecting a saline solution containing B+S, muscimol, or glycine, we injected the same volume (110 μl) of saline alone. The initial injections were made bilaterally into the preBötC ($n = 6$), and 20 min later into the preBötC+BötC ($n = 6$) in vagotomized rats. Respiratory parameters were measured before and 2 min after preBötC injections, then before and 2 min after preBötC+BötC injections (Table 1).

B+S injections (Groups 4–6). B+S were injected using micropipettes (~40 μm tip), bilaterally into the preBötC and then BötC; it took 6–10 min to complete four injections. The volume of each of the four B+S injections was 110 μl. All injections were made using a series of pressure pulses (Picospritzer; Parker-Hannifin) applied to the open
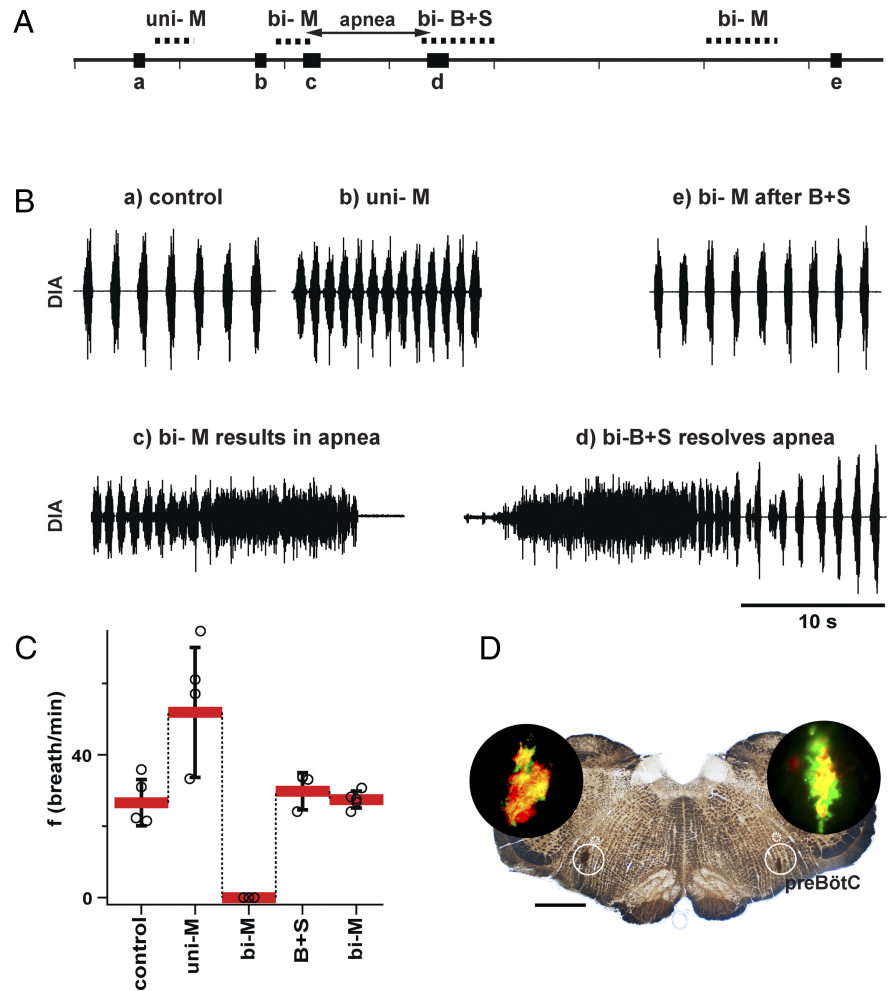

Figure 2. $GABA_A$ receptors in the preBötC were effectively blocked by B+S microinjections (vagotomized rats, $n = 5$). **A**, Timeline of experiment to test potency of B+S injection to block $GABA_A$ receptors. The experiment included recordings under the following sequential conditions: (a) control after bilateral vagotomy; (b) after unilateral injection of muscimol (M; $GABA_A$ agonist) into one preBötC (uni-M); (c) after apnea induced by bilateral injection of muscimol into the preBötC (bi-M); (d) after apnea was resolved by bilateral injection of B+S into the same place as muscimol (bi-B+S); (e) after the second bilateral injection of muscimol into preBötC (bi-M). The same dose of muscimol that resulted in apnea before bi-B+S did not suppress breathing after bi-B+S. **B**, Diaphragmatic activity at critical moments of an experiment described above. **C**, Breathing frequency (mean ± SD; individual data points for each rat) under the above-described conditions. **D**, Transverse section at the level of preBötC. In bright field, FluoSpheres are visible as a darkened area in white circles marking the preBötC. In dark field (DAPI filter cube), the presence of three different fluorescent dyes within one slice is visible (black circle inserts). The small white circle (dotted line) encompasses the subcompact part of nucleus ambiguous. Three consecutive injections (M, B+S, M) were close to each other. Scale bar, 1 mm.

end of micropipettes. Air pressure was set to make each pulse eject ~5 nl, with each of the four injections totaling 110 μl.

The preBötC+BötC spans ~1.3 mm. After collecting data for analysis, in more than half of rats we performed two additional injections within the preBötC+BötC on each side. Injections were placed "in between" the original ones to test whether there was any advantage to covering the preBötC+BötC with four injections per side instead of two injections per side; there was no additional respiratory response.

Ablation of the BötC (Group 7). We ablated the BötC, a primary source of inhibition to the whole respiratory network (Fedorko and Merrill, 1984; Ezure et al., 2003a,b). Bilateral BötC ablation was done using suction through a hypodermic needle ($n = 5$). The resulting lesion was ~700 μm in diameter and centered at 50 μm caudal to the level of the RRXII, i.e., 300 μm caudal to the cVII and 2100 μm lateral to the midline. All tissue ventral to Asc was removed bilaterally. When blood vessels on the surface of the medulla prevented perpendicular placement of the suction needle, we approached the BötC at an angle from a more medial position. Ablation extended ~300 μm rostral and 400 μm caudal to the RRXII and resulted in total destruction of the BötC in every rat (Fig. 8). There was
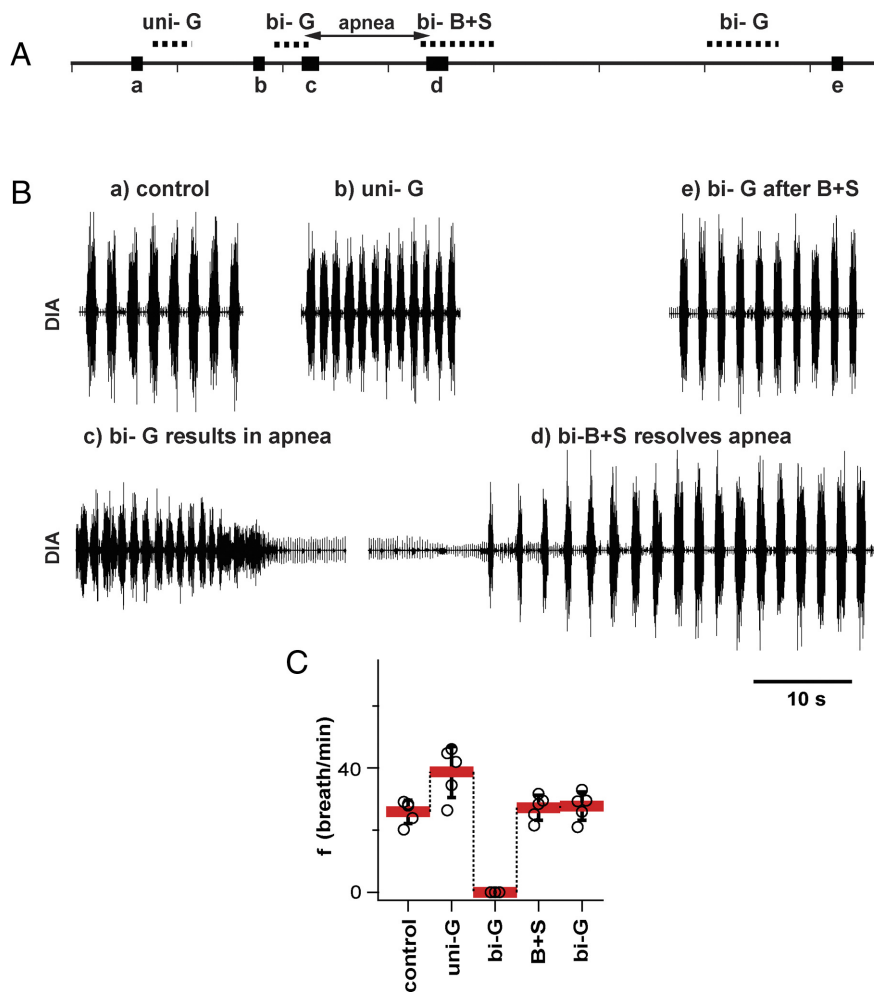
Figure 3. Glycine receptors in preBötC were effectively blocked by B + S microinjections (vagotomized rats; $n = 5$). **A**, Timeline of experiment to test the potency of B + S injection to block glycinergic receptors; similar to Figure 2. The experiment included recordings under the following conditions: (a) control after bilateral vagotomy; (b) after unilateral injection of glycine into one preBötC (uni-G); (c) after apnea induced by bilateral injection of glycine into preBötC (bi-G); (d) after apnea was resolved by bilateral injection of B + S into the same place as glycine (bi-B+S); (e) after the second bilateral injection of glycine (bi-G). The same dose of glycine that resulted in apnea before bi-B + S did not suppress breathing after bi-B + S. **B**, Diaphragmatic activity at critical moments of an experiment described above. **C**, Breathing frequency (mean ± SD; individual data points for each rat) under the above-described conditions.

expiration (postinspiration) to reduce expiratory flow and thus slow the emptying of the lungs. Axons forming the RLN are a part of the cervical vagus, then branch off the vagus nerve at the thoracic level to ascend to the larynx. RLN activity can be recorded from the RLN proper or from the cut trunk of the cervical vagus. The latter method is typically used in an *in situ* perfused preparation (Fong and Potts, 2006; Smith et al., 2007). This activity is commonly used as an indicator of the post-I activity (Fong and Potts, 2006; Smith et al., 2007; Bautista et al., 2012). However, post-I activity critically depends on experimental conditions (Gesell and White, 1938) and can be quite variable in different rats studied under the same experimental conditions (Bautista et al., 2012). The inspiratory component of RLN activity was quantified as the maximum value of the integrated RLN signal during inspiration, i.e., when air was flowing into the lungs. The post-I component of the RLN activity was quantified as the maximum value of the integrated RLN signal after the reversal of airflow from inspiratory to expiratory (Bautista et al., 2012). Respiratory variables, e.g., duration of inspiration, expiration, frequency, tidal volume, and amplitude of integrated EMG, are reported as averages during 20 consecutive cycles. Data for analysis were collected starting at 2–8 min after completion of injections. We compared means using one-way repeated-measures ANOVA followed by all pairwise multiple comparison procedures (Tukey test; SigmaPlot 12; Systat Software). We report the F statistics from repeated-measures ANOVA as $F_{(df_{BT}, df_R)} = F$ value, where df_{BT} is the degrees of freedom between subjects and df_R is the degrees of freedom for residuals. $df_{BT} = k - 1$, where k is the number of repetitions (treatments/conditions), and $df_R = (k - 1)(n - 1)$, where n is the number of rats in a group. For example, Group 4 consisted of seven rats, and frequency was measured (1) before vagotomy, (2) after injection of B+S, and (3) after vagotomy (Table 2). Degrees of freedom $df_{BT} = k - 1 = 3 - 1 = 2$ and $df_R = (k - 1)(n - 1) = 12$. $F_{(2,12)}$ is reported. A value of $p < 0.05$ was considered significant, and p and F values were rounded off to three decimals. Mean cycle durations (T_C) were compared whenever differences in f were evaluated, because f values ($f = 1/T_C$) are not normally distributed. Results are expressed as mean ± SD.

Analysis of the strength of the Breuer–Hering inflation reflex. "Expansion of the lung reflexly inhibits inspiration and promotes expiration, the more strongly the greater the expansion. This effect depends on the integrity of the N. vagus; the fibers affecting the medulla oblongata in this manner run along its path" (Breuer, 1868, page 366 of English translation). Here, the Breuer–Hering inflation reflex (BHIR) was triggered by inflating the lungs using constant positive air pressure (CPAP; +10 cm H_2O). The strength of the BHIR (SBHIR) was evaluated by measuring the duration of the resultant inflation-induced apnea (T_{E-INF}). CPAP was terminated after the reflex was "broken," i.e., when inspirations reappeared despite CPAP. To avoid repeated exposure of spontaneously breathing rats to apneas >30 s, if T_{E-INF} was >30 s, CPAP was reduced to 9.5, 9.0, or 8.5 cm H_2O, until T_{E-INF} was <30 s. SBHIR (Fig. 5A) was calculated as an average of $[(T_{E-INF}/T_{E-CON}) - 1]$ of three repetitions of the reflex, where T_{E-CON} is the expiratory duration during the control period immediately preceding CPAP.

some collateral damage to the Asc and the facial nucleus. Surgical lesions typically affect adjacent tissue due to damaged vascularization and local hemorrhage; thus the "effective" area of ablation might have been larger than revealed by tissue examination.

Recording and analysis of respiratory parameters. The trachea was cannulated and connected to a pneumotachograph (GM Instruments). A flow calibration and calculation of tidal volume (V_T) was performed after every experiment. Flow was digitally integrated to obtain V_T. Electromyogram (EMG) wire electrodes (Cooner Wire) were implanted into the diaphragm to record EMGs. The RLN was dissected from the larynx and placed on a bipolar silver electrode. Intratracheal pressure was measured. Signals were sampled at 2 kHz (Powerlab 16SP; AD Instruments). Activity of the diaphragm and the RLN nerve were recorded, rectified, and digitally integrated to obtain moving averages. Signals presented in Figures 4–7 were integrated with a time constants of 0.1 s. A time constant of 0.01 s was used to measure RLN amplitude during inspiration and postinspiration to more clearly delineate the onset of post-I activity (Bautista et al., 2012). Signals were analyzed using LabChart Pro 7.3.2 (AD Instruments) and Igor Pro 6 (Data Matrix) software. The RLN innervates laryngeal abductor muscles that are active during inspiration to reduce airflow resistance in the larynx. The RLN also innervates laryngeal adductor muscles that increase laryngeal resistance during the first part of

Table 1. Control injections; respiratory parameters in response to agonist–antagonist–agonist and saline injections into the preBötC

	f (breaths/min)	V_T (ml)	T_I (s)	T_E (s)
Group 1 ($n = 5$)				
	26.6 ± 6.5	3.9 ± 0.5	0.7 ± 0.2	1.7 ± 0.3
a: Control	a = c = d	a = c = d	a = b = c = d	a = c = d
	$F_{(2,8)}$ = 1.029; p = 0.400	$F_{(2,8)}$ = 4.348; p = 0.053	$F_{(3,12)}$ = 2.562; p = 0.104	$F_{(2,8)}$ = 3.259; p = 0.092
b: Excitatory response to M	51.9 ± 18.2	2.3 ± 0.7	0.6 ± 0.1	0.7 ± 0.4
	b > a = c = d	b < a = c = d		b < a = c = d
	$F_{(3,12)}$ = 12.887; p = 0.001	$F_{(3,12)}$ = 27.874; p = 0.001		$F_{(3,12)}$ = 17.101; p = 0.001
c: M + (B+S)	29.8 ± 5.2	3.5 ± 0.7	0.6 ± 0.3	1.5 ± 0.1
	c = d (p = 0.900)	c = d (p = 0.982)		c = d (p = 0.625)
d: M + (B+S) + M	27.5 ± 2.4	3.4 ± 0.7	0.5 ± 0.2	1.7 ± 0.3
Group 2 ($n = 5$)				
	25.9 ± 3.8	3.9 ± 0.4	0.8 ± 0.2	1.6 ± 0.3
a: Control	a = c = d	a = c = d	a = b	a = c = d
	$F_{(2,8)}$ = 0.884; p = 0.450	$F_{(2,8)}$ = 0.917; p = 0.438	$F_{(1,4)}$ = 3.152; p = 0.150	$F_{(2,8)}$ = 0.859; p = 0.459
b: Excitatory response to G	38.8 ± 8.2	2.2 ± 0.4	0.7 ± 0.2	0.9 ± 0.3
	b > a = c = d	b < a = c = d	b = a > c = d	b < a = c = d
	$F_{(3,12)}$ = 19.798; p = 0.001	$F_{(3,12)}$ = 26.936; p = 0.001	$F_{(3,12)}$ = 10.727; p = 0.001	$F_{(3,12)}$ = 29.704; p = 0.001
c: G + (B+S)	27.2 ± 4.0	3.6 ± 0.4	0.6 ± 0.1	1.7 ± 0.4
	c = d; p = 0.992	c = d; p = 0.981	c = d; p = 0.988	c = d; p = 0.833
d: G + (B+S) + G	27.7 ± 4.5	3.7 ± 0.5	0.6 ± 0.1	1.7 ± 0.3
Group 3 ($n = 6$)				
	30.3 ± 4.5	4.1 ± 0.7	0.5 ± 0.2	1.5 ± 0.4
a: Before saline injection into preBötC	a = b = c = d	a = b = c = d	a = b = c = d	a = b = c = d
	$F_{(3,15)}$ = 0.801; p = 0.512	$F_{(3,15)}$ = 1.077; p = 0.389	$F_{(3,15)}$ = 2.562; p = 2.262	$F_{(3,15)}$ = 1.300; p = 0.311
b: 2 min after saline injection into preBötC	30.6 ± 5.3	3.9 ± 0.5	0.5 ± 0.1	1.5 ± 0.4
c: Before saline injection into preBötC+BötC	30.8 ± 5.4	4.0 ± 0.5	0.5 ± 0.1	1.5 ± 0.4
d: 2 min after saline injection into preBötC+BötC	31.7 ± 5.0	3.6 ± 0.6	0.5 ± 0.1	1.4 ± 0.4

The F statistics from repeated-measures ANOVA are reported as $F_{(df_{BT}, df_R)}$ = F value, where df_{BT} is the degrees of freedom between subjects, and df_R is the degrees of freedom for residuals. ANOVA was followed by all pairwise multiple comparison procedure (Tukey test). Notation a = b= c means that when a respiratory parameter was measured in the same group of rats under conditions a, b, and c, the differences in the mean values were not great enough to exclude the possibility that the difference was due to random sampling variability, i.e., means were not statistically different. Notation a > b = c means that a null hypothesis that the data under conditions a, b, and c were sampled from populations with the same mean was rejected, and subsequent pair comparison (Tukey test) established that the mean value under condition a is greater than under condition b, while mean values under conditions b and c are not significantly different. M, Muscimol; G, glycine.

Table 2. Respiratory parameters in response to vagotomy, B+S injections (Groups 4 and 5), and BötC ablation (Group 7)

	f (breath/min)	V_T (ml)	T_I (s)	T_E (s)
Group 4 ($n = 7$)				
	71.6 ± 5.0	2.0 ± 0.5	0.3 ± 0.1	0.5 ± 0.1
a: Vagi intact	a > b > c	a < b = c	a < b = c	a < b < c
	$F_{(2,12)}$ = 90.470; p = 0.001	$F_{(2,12)}$ = 124.428; p = 0.001	$F_{(2,12)}$ = 21.548; p = 0.001	$F_{(2,12)}$ = 44.305; p = 0.001
	a > b; p = 0.001	a < b; p = 0.001	a < b; p = 0.002	a < b; p = 0.001
	a > c; p = 0.001	a < c; p = 0.001	a < c; p = 0.001	a < c; p = 0.001
b: Vagi intact plus B+S	34.4 ± 3.7	3.8 ± 0.6	0.5 ± 0.1	1.3 ± 0.2
	b > c; p = 0.004	b = c; p = 0.940	b = c; p = 0.205	b < c; p = 0.032
c: Vagotomized	28.2 ± 4.2	4.1 ± 0.3	0.6 ± 0.1	1.6 ± 0.4
Group 5 ($n = 6$)				
	66.0 ± 6.1	2.2 ± 0.5	0.3 ± 0.1	0.6 ± 0.1
a: Vagi intact	a > b = c	a < b = c	b > a = c	a < b = c
	$F_{(2,10)}$ = 104.057; p = 0.001	$F_{(2,10)}$ = 43.733; p = 0.001	$F_{(2,10)}$ = 43.370; p = 0.001	$F_{(2,10)}$ = 14.173; p = 0.001
	a > b; p = 0.001	a < b; p = 0.001	a < b; p = 0.001	a < b; p = 0.001
	a > c; p = 0.001	a < c; p = 0.001	a = c; p = 0.070	a < c; p = 0.001
b: Vagotomized	29.6 ± 4.0	4.2 ± 0.3	0.7 ± 0.1	1.3 ± 0.3
	b = c; p = 0.483	b = c; p = 0.095	b > c; p = 0.001	b = c; p = 0.096
c: Vagotomized plus B+S	33.0 ± 8.6	3.7 ± 0.7	0.5 ± 0.1	1.5 ± 0.5
Group 7 ($n = 5$)				
	67.8 ± 5.1	2.5 ± 0.6	0.3 ± 0.1	0.6 ± 0.1
a: Vagi intact	a = b; $F_{(1,4)}$ = 0.163; p = 0.707	a = b; $F_{(1,4)}$ = 0.836; p = 0.412	a = b; $F_{(1,4)}$ = 2.647; p = 0.179	a = b; $F_{(1,4)}$ = 4.341; p = 0.106
b: Vagi intact plus BötC ablation	74.0 ± 17.4	2.2 ± 0.7	0.4 ± 0.2	0.4 ± 0.1

For details, see Table 1 legend.

Histological processing. Histological examination was used to determine injection placement and, in Group 7, whether the BötC was completely ablated. Rats were perfused and the brainstem removed and sectioned. Freshly cut wet tissue (50 μm coronal or sagittal sections) was photographed under white light to locate the FluoSpheres (Invitrogen) in relation to landmark structures (cVII, Asc, Ac, LRN; Fig. 1). Under white light, FluoSpheres were visible as darker (less transparent) spots (Figs. 1B, 2D). Distances from cVII, Asc, and Ac were measured. In all cases,
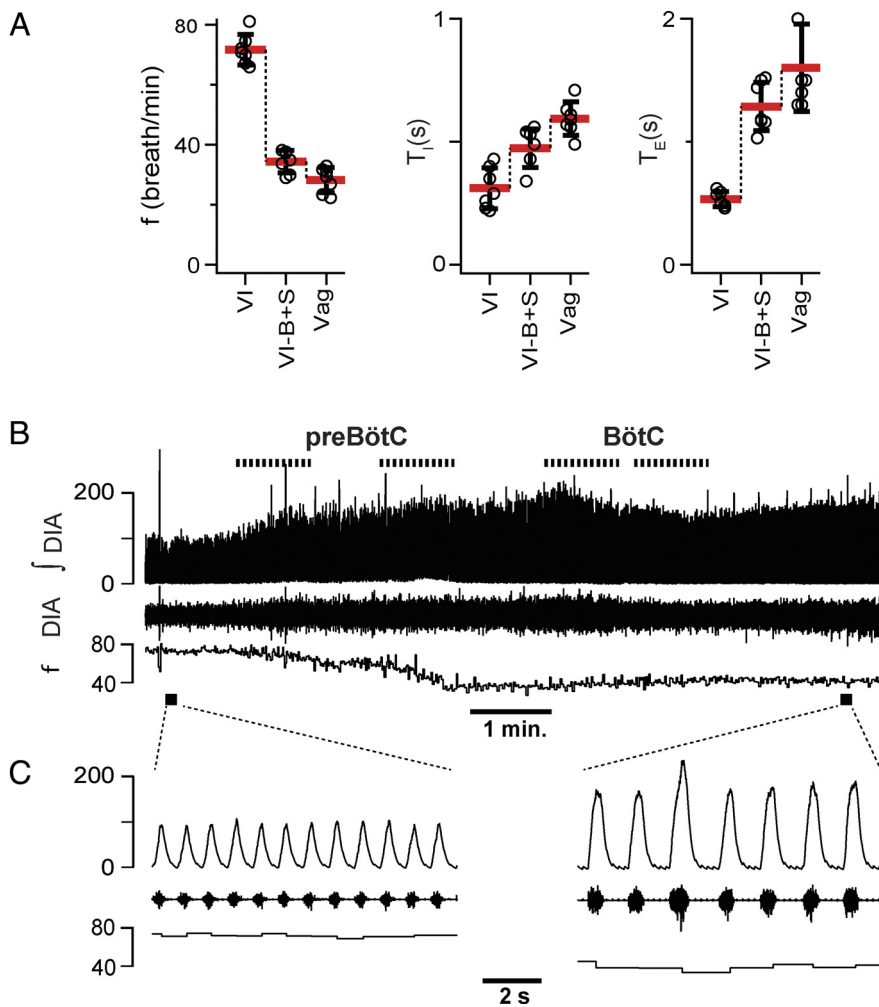
Figure 4. B+S microinjection within the preBötC and BötC did not result in apnea in vagus-intact rats ($n = 7$). **A**, Breathing frequency (f), duration of inspiration (T_I), and duration of expiration (T_E) measured under three different conditions: control/vagi intact (VI), after administration of B+S (VI-B+S), and after subsequent vagotomy (Vag). **B**, Diaphragm EMG activity and f during B+S injections. Top to bottom: Markers of injections; traces of integrated activity of the diaphragm ($\int$DIA), raw activity of the diaphragm (DIA), and f; markers of expanded traces. **C**, Expanded traces in control and after B+S injections.

Results

Control experiments: (B+S) microinjections into preBötC effectively blocked GABA$_A$ and glycine receptors (Groups 1 and 2)

We performed controls to confirm the effectiveness of blocking GABA$_A$ and glycine receptors at target sites (Figs. 2, 3). In anesthetized vagotomized rats, a micropipette filled with the GABA$_A$ agonist muscimol (95 μM) was placed into the preBötC on each side ($n = 5$; Group 1). A sequence of pressure pulses (~5 nl) ejected 90 nl muscimol solution per side, with bilateral injections producing apnea (during which time the rats were mechanically ventilated). After a unilateral muscimol injection, f increased to 200.1 $\pm$ 83.7% ($F_{(1,4)} = 20.985$; $p = 0.010$; $n = 5$), and V_T dropped to 58.9 $\pm$ 14.5% ($F_{(1,4)} = 37.674$; $p = 0.004$) of preinjection values. After bilateral injection, a similar increase in f was followed by low amplitude irregular bursting, then by tonic activity and apnea (Fig. 2Bc, C). We then replaced both muscimol pipettes at the same ejection sites with ones containing B+S (238 μM each). After 5–6 min of muscimol-induced apnea, we injected B+S (110 nl per side). Diaphragmatic activity and associated breathing movements reappeared (Fig. 2Bd, C), and rats were disconnected from the ventilator. Ten minutes later, bilateral injection of muscimol (identical to the one that caused apnea; 95 μM, ~90 nl per side) did not suppress breathing (Fig. 2Be, C; Table 1). FluoSpheres of different colors were added during the first and second injections of muscimol and for the injection of B+S. The overlap of these distinct markers confirmed that all three injections were made within the preBötC (Fig. 2D). Group mean values of f in the control, after muscimol with B+S, and after muscimol with B+S and a second injection of muscimol were 26.6 $\pm$ 6.5, 29.8 $\pm$ 5.2, and 27.5 $\pm$ 2.4 breaths per minute, respectively; they did not differ [$F_{(2,8)} = 1.029$; not significant (n.s.); $p = 0.400$].

In a separate group of rats, we repeated this protocol with glycine (5.7 mM; Group 2; Fig. 3). Glycine-induced apnea was also preceded by an increase in f (Fig. 3Bb, C). After a unilateral injection, f increased to 149.4 $\pm$ 22.9% ($F_{(1,4)} = 41.851$; $p = 0.003$; $n = 5$) and V_T dropped to 57.4 $\pm$ 6.6% ($F_{(1,4)} = 328.942$; $p = 0.001$) of preinjection values (Table 1). Bilateral injection of glycine (110 nl per side) induced apnea, at which point rats were ventilated. Glycine-induced apnea lasted >4 min ($n = 5$). Apnea

these beads were found to be close (<70 μm) to the center of the preBötC or BötC. They were in the same parasagittal plane as the Ac and 330 $\pm$ 50 μm caudal to the cVII and 260 $\pm$ 50 μm ventral to the Ac for BötC injections, and in the same parasagittal plane as the Asc and 1000 $\pm$ 70 μm caudal to the cVII and 260 $\pm$ 50 μm ventral to the Asc for preBötC injections.

Reelin is an effective marker for the preBötC (Tan et al., 2012); therefore, evaluation using freshly cut wet tissue was followed by double-DAB staining for reelin and choline acetyltransferase (ChAT; Fig. 1C) to confirm the accuracy of our method of finding preBötC/BötC using fresh cut sagittal slices. Slices were photographed again after a double-DAB staining. We determined that during processing, sagittal slices shrunk, on average, to 87% in the rostrocaudal direction and to 84% in the dorsoventral direction of their dimensions after cutting (Fig. 1B). For comparison, Paxinos at al. (1999) reported homogenous shrinkage to 81% of thinner (31 μm) coronal slices at the level of the preBötC. After compensation for the shrinkage by a factor of 1.15 in the rostrocaudal direction and 1.2 in the dorsoventral direction (Photoshop, Adobe), images of stained and fresh slices could be overlapped to check location of the FluoSpheres in relation to reelin positive neurons marking the preBötC. We found that using the Ac, Asc, and cVII as landmarks, and by measuring distance from the cVII, the preBötC can be located with similar accuracy using fresh and processed tissue. Antibodies were used in the following sequence: (1) primary antibody (1:500; anti-reelin; amino ac-

was reversed by bilateral B+S injections (238 μM each, 110 nl per side). A subsequent bilateral injection of the same dose of glycine that previously caused apnea (110 nl; 5.7 mM) did not result in apnea (Fig. 3Be; Table 1). Group mean values of f in the control, after glycine with B+S, and after glycine with B+S and a second injection of glycine were 25.9 ± 3.8, 27.2 ± 4.0, and 27.7 ± 4.5 breaths per minute, respectively; they did not differ ($F_{(2,8)} = 0.884$; n.s.; $p = 0.450$; $n = 5$).

We also tested the effect of injecting vehicle (saline) on breathing parameters. We injected 110 μl of saline first bilaterally into the preBötC alone, and 20 min later into the preBötC+BötC in six vagotomized rats. A single pressure pulse affected rhythm for less than five cycles. The depression of f during multiple pressure pulses necessary to inject 110 μl of saline varied from rat to rat. Critically, there was no significant difference in breathing just before and 2 min after bilateral injection of saline into the preBötC. There was no significant difference before and 2 min after completion of injections into the preBötC then BötC (Table 1; Group 3). Moreover, four series of measurements, (1) before and (2) 2 min after preBötC injections and (3) before and (4) 2 min after preBötC+BötC injections, were not statistically different (Table 1). Thus, any insult to the preBötC+BötC related to pressure pulses or to saline itself subsided within 2 min postinjection. Consequently, we collected data 2–8 min after injection.

Block of inhibition in preBötC and BötC did not result in apnea but suppressed BHIR in vagus-intact rats (Group 4)
B+S was injected bilaterally into the preBötC then the BötC (Figs. 4–7; Table 2). These four injections were completed within 6–10 min. In rats with intact vagi, f dropped to $49.7 \pm 6.3\%$ ($F_{(1,6)} = 135.859$; $p = 0.001$; $n = 7$) of control (i.e., preinjection) value. T_I increased to $190.4 \pm 29.5\%$ ($F_{(1,6)} = 181.104$; $p = 0.001$) and expiratory duration (T_E) increased to $228.3 \pm 69.2\%$ ($F_{(1,6)} = 34.699$; $p = 0.001$) of control (Fig. 4A). Subsequent vagotomy decreased f to $81.7 \pm 7.8\%$ ($F_{(1,6)} = 26.510$; $p = 0.002$) of that after B+S injections, did not change T_I ($F_{(1,6)} = 0.106$; $p = 0.755$), and further increased T_E to $139.2 \pm 13.7\%$ of that after B+S injections ($F_{(1,6)} = 51.790$; $p = 0.001$; Fig. 4A).

We further investigated why block of inhibition decreased f and increased T_I and T_E in rats with intact vagi. Since vagotomy also slowed f, we tested the effect of block of inhibition on the BHIR, a powerful lung inflation-induced, vagally mediated reflex that requires fast synaptic inhibition within the medulla (Ezure
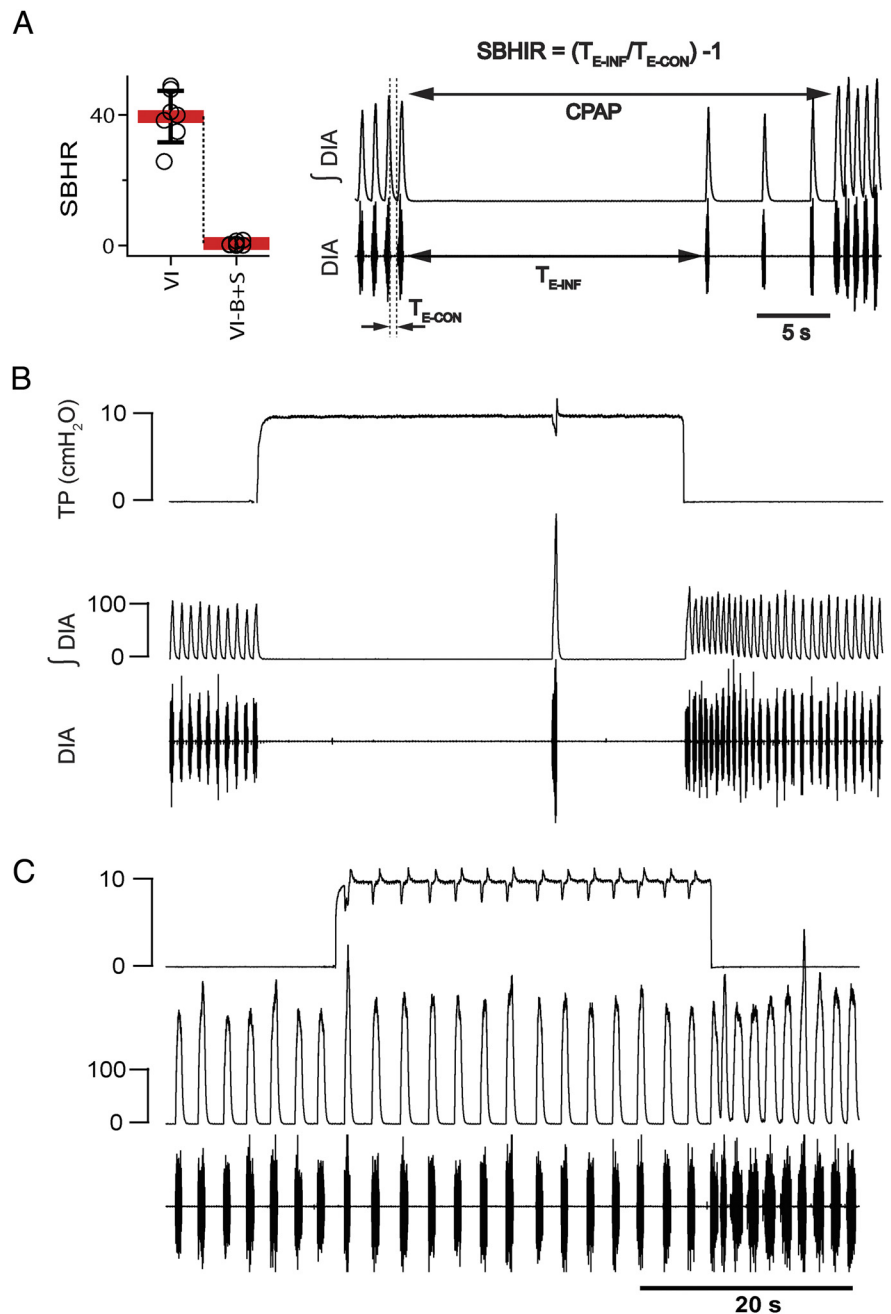

Figure 5. B+S microinjection within the preBötC and BötC suppressed BHIR ($n = 7$). **A**, The SBHIR measured before and after B+S microinjection into preBötC. The right panel explains how SBHIR was calculated. $T_{E\text{-INF}}$ is a period between two consecutive inspirations when lungs are inflated using CPAP (10 cm H_2O); $T_{E\text{-CON}}$ is a period between inspirations without CPAP. SBHIR is a ratio between $T_{E\text{-INF}}$ and $T_{E\text{-CON}}$ minus 1. **B**, In control [vagi intact (VI)], lung inflation resulted in apnea lasting $T_{E\text{-INF}} = 27.7$ s and SHBIR = 42. **C**, BHIR suppressed by B+S within preBötC+BötC (VI-B+S). Lung inflation did not result in apnea and SHBIR = 0.38, <1% of control value. Traces in **B** and **C** (top to bottom) represent tracheal pressure (TP) and integrated ($\int$DIA) and raw (DIA) electromyograms of the diaphragm.

and Tanaka, 2004; Mellen et al., 2004; Kubin et al., 2006). If B+S injections suppressed the BHIR (measured by a reduction in the SBHIR; Fig. 5A), this could at least partially explain their effects on f. Apnea induced by lung inflation ($T_{E\text{-INF}}$) ranged from 14.3 to 27.8 s (19.6 ± 3.9 s; $n = 7$), and SBHIR from 25.7 to 48.9 (39.5 ± 7.9; $n = 7$; Fig. 5A) before B+S. After bilateral B+S injection, the BHIR was effectively eliminated (Fig. 5C): $T_{E\text{-INF}}$ was reduced to 1.8 ± 0.9 s (range, 0.8 to 3.2 s), which was 9.4 ± 5% of its preinjection value ($F_{(1,6)} = 206.080$; $p = 0.001$; $n = 7$; Fig. 5, compare B, C); SBHIR was 0.6 ± 0.6 (range, 0.07 to 1.6),
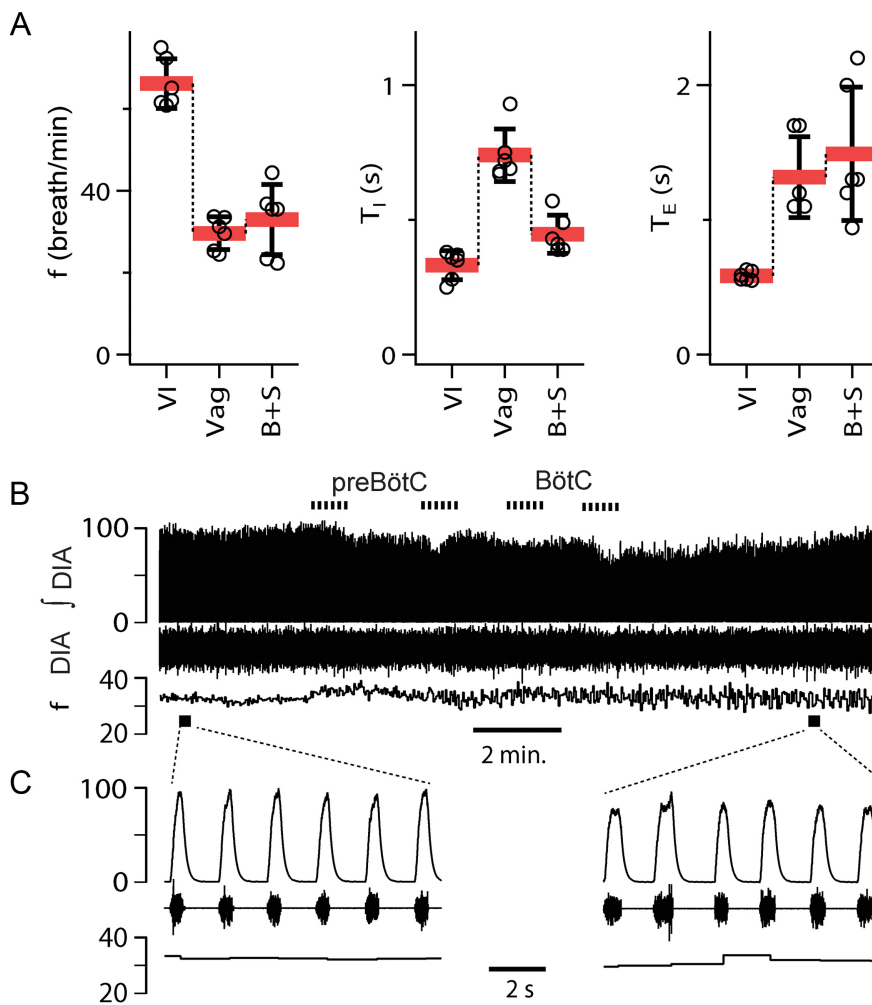
Figure 6. Breathing frequency unaffected by B+S microinjection within preBötC and BötC in vagotomized rats ($n = 6$). ***A***, Breathing frequency (f), duration of inspiration (T_I), duration of expiration (T_E) in three different conditions: control/vagi intact (VI), after subsequent vagotomy (Vag), and after administration of B+S. B+S was injected bilaterally into preBötC then BötC (B+S; mean ± SD, individual data points for each rat). ***B***, Diaphragm EMG activity and f during B+S injections. From top to bottom: Markers of injections; integrated activity of the diaphragm ($\int$DIA), raw activity of the diaphragm (DIA), and f; markers of expanded traces. ***C***, Expanded traces in control and after B+S injections.

Block of inhibition in preBötC and BötC did not eliminate RLN activity in vagus-intact rats (Group 6)

In five additional rats with intact vagi, RLN activity was recorded to determine whether block of inhibition affected post-I activity (Fig. 7). The RLN had inspiratory activity followed by post-I activity during some, but not all, respiratory cycles in three of five rats before injection; in two of five rats there was no preinjection post-I activity, only tonic activity during expiration. After B+S, inspiratory RLN activity increased to 342.2 ± 151.7% ($F_{(1,4)} = 12.781$; $p = 0.023$; $n = 5$), and f dropped to 52.6 ±7.4% ($F_{(1,4)} = 84.259$; $p = 0.001$; $n = 5$; Fig. 7) of control. Block of inhibition did not eliminate post-I or tonic expiratory activity ($n = 5$). In the three rats that had post-I activity during control, it increased to 730.9 ± 231.1% ($F_{(1,2)} = 22.379$; $p = 0.042$; $n = 3$) of control.

Bilateral ablation of BötC did not result in apnea, nor did it abolish the BHIR in vagus-intact rats (Group 7)

The BötC contains post-I and aug-E inhibitory neurons (Ezure et al., 2003a,b). In the inhibitory ring model, these neural populations are hypothesized to be essential for normal rhythmogenesis (Smith et al., 2007; Molkov et al., 2010). Bilateral ablation of the BötC was done by exposing the ventral brainstem surface and removing the BötC by suction through a hypodermic needle ($n = 5$; Fig. 8C). Histological analysis confirmed ablation of the BötC plus, presumably, some surrounding tissue. Nonetheless, f did not change (109.9 ± 29.9% of control; $F_{(1,4)} = 0.163$; n.s.; $p = 0.707$), T_I had a tendency to increase (142.9 ± 38.4% of control; $F_{(1,4)} = 2.647$; n.s.; $p = 0.179$), and T_E had a tendency to decrease (72.5 ± 17.6% of control; $F_{(1,4)} = 4.341$; n.s.; $p = 0.106$; Table 2, Fig. 8A). SBHIR was unaffected, equal to 43.1 ± 2.7 before and 48.4 ± 8.4 after ablations ($F_{(1,4)} = 1.904$; n.s.; $p = 0.240$; Fig. 8A).

Discussion

Inhibition is critical to all aspects of nervous system function. Approximately half of the neurons in the preBötC (Winter et al., 2009) and most of the neurons in the BötC (Merrill, 1981; Fedorko and Merrill, 1984; Ezure et al., 2003a,b) are inhibitory. We hypothesized that in the intact mammal, inhibition modulates breathing frequency and can induce apnea, but is not required for rhythmogenesis underlying normal breathing, i.e., eupnea, per se. We tested this hypothesis in the adult anesthetized rat by blocking inhibition within the preBötC, which contains neurons critical for rhythmogenesis (Smith et al., 1991; Gray et al., 1999; Tan et al., 2008), and the BötC, a primary source of inhibition to the respiratory network (Merrill, 1981; Fedorko and Merrill, 1984; Feldman et al., 1984; Ezure et al., 2003a,b). We found that following block of $GABA_A$ and glycinergic receptors at

which was only 1.5 ± 1.5% ($F_{(1,6)} = 177.410$; $p = 0.001$) of its value before the block. A drop of SBHIR to <2% of its control value is comparable to the effect of blocking pulmonary stretch receptors (Davies et al., 1978). This finding links SBHIR to inhibition within preBötC+BötC and is a positive control for the effectiveness of the B+S injections.

Block of inhibition in preBötC and BötC did not result in apnea in vagotomized rats (Group 5)

Vagotomy reduced f to 45.2 ± 5.4% ($F_{(1,5)} = 130.973$; $p = 0.001$; $n = 6$) of that before vagotomy, i.e., with vagi intact (Fig. 6A; Table 2). After B+S injection, f did not change (112.1 ± 29.9%; n.s.; $F_{(1,5)} = 0.833$; $p = 0.403$) compared to vagotomized controls (Fig. 6A,C). T_I dropped to 61.7 ± 29.9% ($F_{(1,5)} = 22.736$; $p = 0.005$). There was an insignificant trend for T_E to increase to 116.6 ± 44.9% ($F_{(1,5)} = 0.645$; n.s.; $p = 0.458$), while cycle duration ($T_I + T_E$) was the same (95.5 ± 30.6%; $F_{(1,5)} = 0.833$; n.s.; $p = 0.403$) as before B+S injections.

these two sites in vagotomized rats, *f* was unaffected (Fig. 6). In vagus-intact rats, *f* slowed (Figs. 4, 5), which we suggest (see below) is largely a consequence of suppression of the BHIR (Fig. 5). Since B + S injections into preBötC + BötC did not produce apnea (nor apneusis nor gasping) and had no significant effect on *f* in vagotomized rats, we performed two controls to assure that inhibitory neurotransmission mediated by GABA$_A$ and glycine receptors was effectively blocked. Thus, B+S injections could (1) prevent or reverse apnea induced by preBötC injection of a GABA$_A$ergic (muscimol) or a glycinergic (glycine) agonist (Figs. 2, 3), and (2) suppress the BHIR (Fig. 5). The latter effect is a positive control that also confirms a critical role of preBötC+BötC inhibition for the BHIR (Ezure and Tanaka, 2004; Mellen et al., 2004; Kubin et al., 2006) and can mostly account for the substantial reduction in *f* following B+S injections in vagus-intact rats. The increase in RLN activity in response to B+S injections is consistent with suppression of the BHIR, because upper airway nerves (including the RLN) are strongly activated when released from the volume feedback triggering the BHIR (Kuna, 1986). Here, the post-I component of RLN activity increased approximately sevenfold, and the inspiratory component approximately threefold. An increase in post-I activity is consistent with depolarization of post-I neurons when they are released from GABAergic (Haji et al., 1992, their Fig. 6) and glycinergic inhibition (Schmid et al., 1996, their Fig. 5).

The BötC contains post-I and aug-E inhibitory neurons (Ezure et al., 2003a,b; Smith et al., 2007). Ablation of the BötC did not change *f* in vagus-intact rats (Fig. 8). We conclude that the BötC is not necessary for generation of respiratory rhythm; rather, its constituent post-I and aug-E inhibitory neurons modulate activity supplying upper airway muscles that control upper airway resistance and airflow (Abdala et al., 2010).

The BHIR is associated with excitation or inhibition of neurons throughout respiratory column in the medulla and pons (Hayashi et al., 1996; Kubin et al., 2006), including the BötC where post-I inhibitory neurons are excited by lung inflation (Manabe and Ezure, 1988; Fong and Potts, 2006). The persistence of the reflex after BötC lesions indicates that apnea in response to lung inflation requires inhibition within the preBötC, rather than the BötC. In *en bloc* preparations of neonatal rat lacking the pons and with lungs attached and innervated by the right vagus nerve, preBötC inspiratory neurons are hyperpolarized during lung inflation. Furthermore, the BHIR is eliminated by bath application of bicuculline (Mellen et al., 2004, their Figs. 4*Bii*, 10*C*), but not by strychnine (their Fig. 7*Bii*), suggesting that block of GABA$_A$ (rather than glycine) receptors within the preBötC is the most likely mechanism underlying the suppression of the BHIR. Under
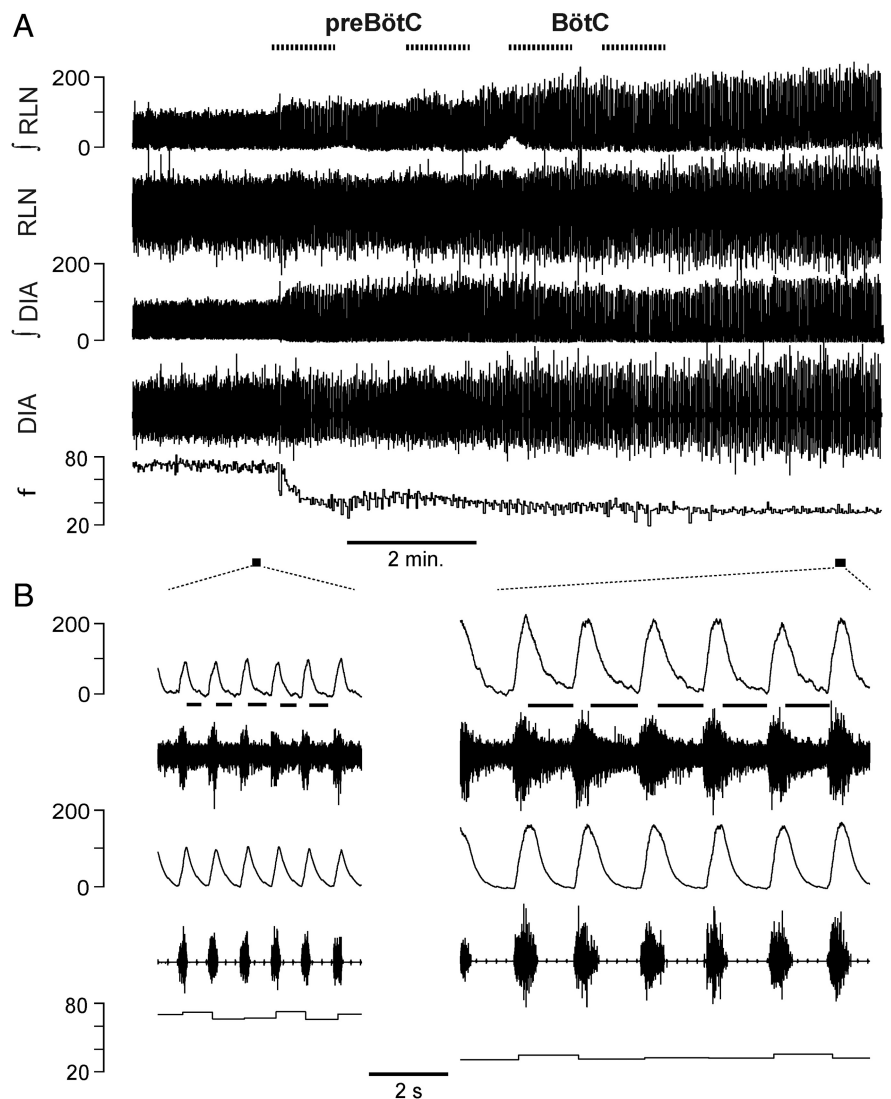

Figure 7. Recurrent laryngeal nerve and diaphragm activity not abolished by B+S injections within the preBötC and BötC in vagus-intact rats (*n* = 5). *A*, Changes in electromyograms and frequency of breathing (*f*) during B+S injections (dotted lines at top). Traces from top to bottom: electromyogram of the RLN and its integral (∫RLN), electromyogram of the diaphragm (DIA) and its integral (∫DIA), *f*, and markers of expanded traces. *B*, Expanded traces during control and after B+S injections. Lines below ∫RLN in the expanded traces mark post-I activity.

control conditions, lung inflation could produce an apnea lasting 19.6 ± 3.9 s (~22 respiratory cycles), but following B+S within the preBötC, this protective reflex was gone (Fig. 5). Since apnea is an important component of many regulatory and protective reflexes (e.g., diving and aspiration reflexes) and other motor acts (e.g., phonation, swallowing, Valsalva maneuver), we hypothesize that inhibition within the preBötC is essential for its production. We predict that B+S injections into the preBötC will markedly alter all of these acts.

The respiratory effects of blocking inhibition in previous studies depended on experimental conditions and whether inhibition was selectively blocked in the ventral respiratory column or within the whole brainstem. In an arterially perfused *in situ* hypothermic brainstem–spinal cord preparation that lacks a functional BHIR, blocking of Cl⁻-mediated inhibition by intra-aortic perfusion with a low Cl⁻ solution stops the rhythm (Hayashi and Lipski, 1992; Smith et al., 2007), and blocking with B+S does not stop the rhythm, which continues but changes in shape and regularity (St-John et al., 2009, their Figs. 1*B*, 2*B*). In brainstem–
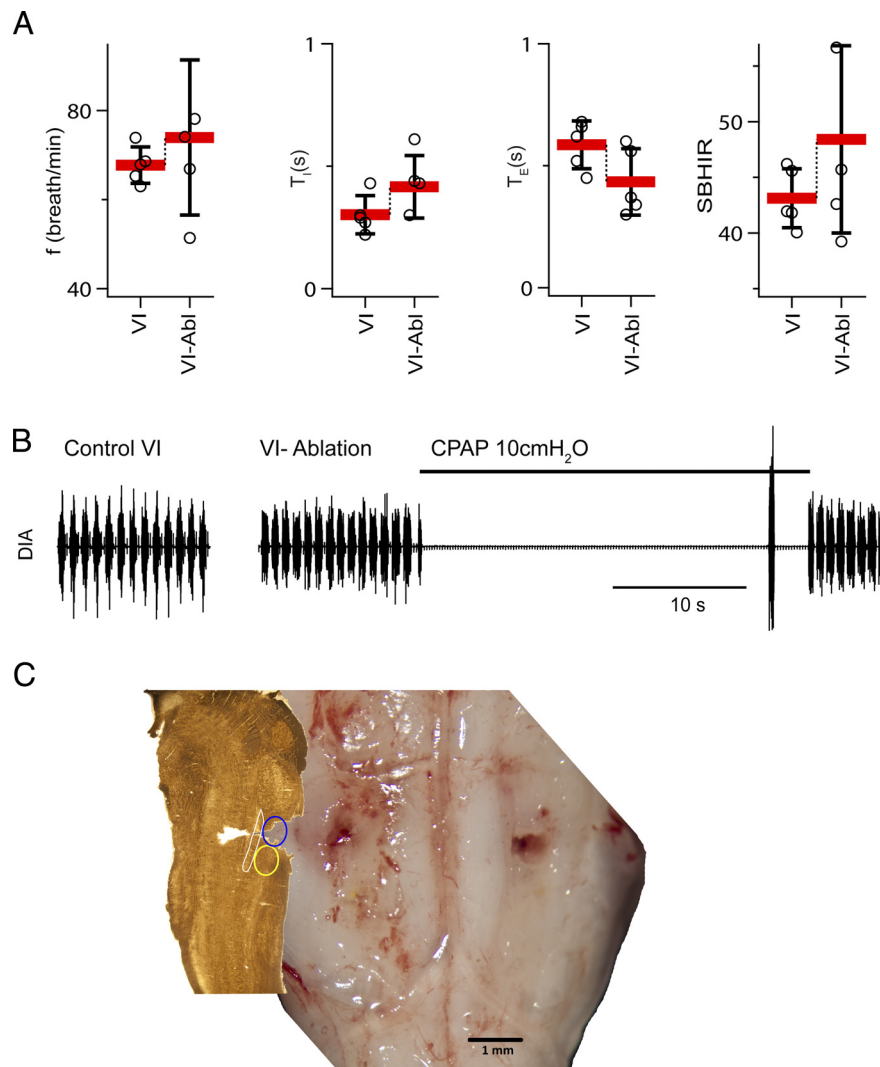
A

B

C

Figure 8. Ablation of the Bötzinger complex did not eliminate respiratory rhythm and did not suppress the BHIR (*n* = 5). ***A***, Breathing frequency (*f*), duration of inspiration (T_I), duration of expiration (T_E), and SBHIR before and after bilateral ablation of the BötC in rats with vagi intact (VI). Ablation (Abl) of BötC did not diminish SBHIR (mean ± SD; individual data points for each rat). ***B***, Activity of the diaphragm before and after bilateral BötC ablation. ***C***, Histological verification of the BötC lesion. Left, Parasagittal section cut at 2.1 mm from the brainstem presented at the right. The blue ellipse is the presumptive location of the ablated BötC. The yellow ellipse indicates position of the preBötC.

With the noted exception of pacemaker and group-pacemaker models (Feldman and Smith, 1989; Rubin et al., 2009), respiratory rhythm generation is generally postulated to critically rely on inhibition between two or three groups of neurons (Lumsden, 1923; Burns, 1963; Richter, 1982; von Euler, 1983; Richter et al., 1992; Smith et al., 2007, 2012). Results from a perfused *in situ* preparation led to a model where rhythm is generated by an "inhibitory ring" of three distinct neural populations that sequentially inhibit each other. In this model under normal resting conditions, excitatory preBötC neurons remain in a "tonic activity mode" and do not generate rhythm, but rather provide tonic drive that is periodically inhibited by the inhibitory ring (Smith et al., 2007; Molkov et al., 2010). When the preBötC is isolated from more rostral structures, e.g., in the rhythmic slice, the preBötC is postulated to take over generation of the rhythm by a different, pacemaker-driven mechanism ("intrinsic bursting mode") characterized by low frequency, decrementing inspiratory bursts, and absence of the post-I activity (Smith et al., 2007; St-John et al., 2009).

Could our results be explained by a rapid transformation from an inhibition-dependent rhythm to a pacemaker-driven rhythm? It is unlikely, as we did not observe a slow decrementing inspiratory motor pattern (nor gasping nor apneusis; Figs. 4-7), nor was post-I activity eliminated (Fig. 7) when inhibitory blockade was confined to sites where it could affect rhythmogenesis, i.e., the preBötC and BötC. Our data indicate that the preBötC generates rhythmic inspiratory bursts in the absence of conventional postsynaptic inhibition, with or without vagi and with or without a robust BHIR. These data can be explained by a group-pacemaker model where inspiratory bursts are generated by excitatory glutamatergic neurons endowed with activity-dependent cellular mechanisms enabling burst termination that does not require postsynaptic inhibition (Feldman and Del Negro, 2006; Krey et al., 2010; Feldman et al., 2013). We propose that inhibition, tonic or phasic, modulates burst shape (Younes et al., 1978), resulting in lower amplitude bursts and faster rhythm, as when inhibition within the preBötC was increased by muscimol (Fig. 2*B*, compare a, b) or glycine (Fig. 3*B*, compare a, b), and higher amplitude bursts and slower rhythm after block of inhibition (Figs. 4*C*, compare left, right panels; 7*B*).

We conclude that inhibition within the preBötC and/or BötC is not required for a normal breathing rhythm in the adult anesthetized rat, with or without vagi. We further suggest that this represents a more general principle for the role of inhibition in rhythmogenesis and central pattern generation relevant to other important movements in mammals (Li, 2011), such as locomotion/swimming (Grillner and Jessell,

spinal cord preparations *in vitro* (Feldman and Smith, 1989; Mellen et al., 2004) and medullary slices (Shao and Feldman, 1997) containing the preBötC, the rhythm continues following bath application of inhibitory antagonists. In the chloralose/urethane-anesthetized rabbit, the rhythm continues after injection of bicuculline into the preBötC and BötC (Bongianni et al., 2010, their Figs. 6, 7). Apnea resulting from block of GABA$_A$ergic inhibition within the BötC reverts to regular breathing following an increase in chemical drive (Bongianni et al., 2010, their Fig. 2). In pentobarbital-anesthetized adult cats, bilateral B+S injections into the preBötC can produce apnea (*n* = 5 of 7), but injections into the BötC have no effect on breathing (Pierrefiche et al., 1998, their Fig. 1*A*). The fact that our B+S injections into the adult rat preBötC+BötC did not produce apnea may be due to species differences or, more likely, the additional effect of systemic pentobarbital, a respiratory depressant that significantly potentiates GABA$_A$ergic inhibition (Macdonald and Olsen, 1994) throughout the entire neuraxis, which could bias the effects of transient inhibitory blockade.

2009; Cangiano et al., 2012) or chewing (Gossard et al., 2010). We emphasize that our conclusion does not diminish the importance of inhibition in shaping burst patterns and modulating frequency, control of airway muscles (Abdala et al., 2010), respiratory reflexes, assuring that inspiratory burst termination becomes irreversible (Younes et al., 1978), suppressing spurious excitatory sensory inputs (Feldman and Grillner, 1983), gating active expiration (Pagliardini et al., 2011), and mediating (prolonged) apneas, all essential for proper functioning of the neural circuits driving breathing under real-world conditions in intact mammals.

References

Abdala AP, Beihui HL, Rybak IA, Smith JC, Paton JF (2010) Role of GlyT2 expressing neurons in the Bötzinger complex for respiratory rhythm and pattern generation. FASEB J 24:614.3.

Bautista TG, Xing T, Fong AY, Pilowsky PM (2012) Recurrent laryngeal nerve activity exhibits a 5-HT-mediated long-term facilitation and enhanced response to hypoxia following acute intermittent hypoxia in rat. J Appl Physiol 112:1144–1156. CrossRef Medline

Bongianni F, Mutolo D, Cinelli E, Pantaleo T (2010) Respiratory responses induced by blockades of GABA and glycine receptors within the Bötzinger complex and the pre-Bötzinger complex of the rabbit. Brain Res 1344:134–147. CrossRef Medline

Bradley GW, von Euler C, Marttila I, Roos B (1975) A model of the central and reflex inhibition of inspiration in the cat. Biol Cybern 19:105–116. CrossRef Medline

Breuer J (1868) Self-steering of respiration through the nervus vagus in breathing (in German; E. Ullmann, translator). Reprint: Breathing: Hering-Breuer Centenary Symposium (Pother R, ed), pp 359 -394. London: J. and A. Churchill, 1970.

Brown TG (1914) On the nature of the fundamental activity of the nervous centres; together with an analysis of the conditioning of rhythmic activity in progression, and a theory of the evolution of function in the nervous system. J Physiol 48:18–46. Medline

Burns BD (1963) The central control of respiratory movements. Br Med Bull 19:7–9. Medline

Cangiano L, Hill RH, Grillner S (2012) The hemisegmental locomotor network revisited. Neuroscience 210:33–37. CrossRef Medline

Chitravanshi VC, Sapru HN (2002) Microinjections of glycine into the pre-Bötzinger complex inhibit phrenic nerve activity in the rat. Brain Res 947:25–33. CrossRef Medline

Davies A, Dixon M, Callanan D, Huszczuk A, Widdicombe JG, Wise JC (1978) Lung reflexes in rabbits during pulmonary stretch receptor block by sulphur dioxide. Respir Physiol 34:83–101. CrossRef Medline

Ezure K, Tanaka I (2004) GABA, in some cases together with glycine, is used as the inhibitory transmitter by pump cells in the Hering-Breuer reflex pathway of the rat. Neuroscience 127:409–417. CrossRef Medline

Ezure K, Tanaka I, Kondo M (2003a) Glycine is used as a transmitter by decrementing expiratory neurons of the ventrolateral medulla in the rat. J Neurosci 23:8941–8948. Medline

Ezure K, Tanaka I, Saito Y (2003b) Brainstem and spinal projections of augmenting expiratory neurons in the rat. Neurosci Res 45:41–51. CrossRef Medline

Fedorko L, Merrill EG (1984) Axonal projections from the rostral expiratory neurones of the Bötzinger complex to medulla and spinal cord in the cat. J Physiol 350:487–496. Medline

Feldman JL, Cowan JD (1975) Large-scale activity in neural nets II: a model for the brainstem respiratory oscillator. Biol Cybern 17:39–51. CrossRef Medline

Feldman JL, Del Negro CA (2006) Looking for inspiration: new perspectives on respiratory rhythm. Nat Rev Neurosci 7:232–242. CrossRef Medline

Feldman JL, Grillner S (1983) Control of vertebrate respiration and locomotion: a brief account. Physiologist 26:310–316. Medline

Feldman JL, Smith JC (1989) Cellular mechanisms underlying modulation of breathing pattern in mammals. Ann N Y Acad Sci 563:114–130. CrossRef

Feldman JL, McCrimmon DR, Speck DF (1984) Effect of synchronous activation of medullary inspiratory bulbo-spinal neurones on phrenic nerve discharge in cat. J Physiol 347:241–254. Medline

Feldman JL, Connelly CA, Ellenberger HH, Smith JC (1990) The cardiorespiratory system within the brainstem. Eur J Neurosci [Suppl] 3:17.

Feldman JL, Del Negro CA, Gray PA (2013) Understanding the rhythm of breathing: so near, yet so far. Annu Rev Physiol 75:423–452. CrossRef Medline

Fong AY, Potts JT (2006) Neurokinin-1 receptor activation in Bötzinger complex evokes bradypnoea. J Physiol 575:869–885. CrossRef Medline

Gesell R, White F (1938) Recruitment of muscular activity and the central neurone after-discharge of hyperpnea. Am J Physiol 122:48–56.

Gossard JP, Dubuc R, Kolta A, eds (2010) Breathe, walk and chew: the neural challenge: part I. Amsterdam: Elsevier.

Gray PA, Rekling JC, Bocchiaro CM, Feldman JL (1999) Modulation of respiratory frequency by peptidergic input to rhythmogenic neurons in the preBötzinger complex. Science 286:1566–1568. CrossRef Medline

Grillner S, Jessell TM (2009) Measured motion: searching for simplicity in spinal locomotor networks. Curr Opin Neurobiol 19:572–586. CrossRef Medline

Haji A, Takeda R, Remmers JE (1992) Evidence that glycine and GABA mediate postsynaptic inhibition of bulbar respiratory neurons in the cat. J Appl Physiol 73:2333–2342. Medline

Hayashi F, Lipski J (1992) The role of inhibitory amino acids in control of respiratory motor output in an arterially perfused rat. Respir Physiol 89:47–63. CrossRef Medline

Hayashi F, Coles SK, McCrimmon DR (1996) Respiratory neurons mediating the Breuer-Hering reflex prolongation of expiration in rat. J Neurosci 16:6526–6536. Medline

Kalia M, Feldman JL, Cohen MI (1979) Afferent projections to the inspiratory neuronal region of the ventrolateral nucleus of the tractus solitarius in the cat. Brain Res 171:135–141. CrossRef Medline

Krey RA, Goodreau AM, Arnold TB, Del Negro CA (2010) Outward currents contributing to inspiratory burst termination in preBötzinger Complex neurons of neonatal mice studied in vitro. Front Neural Circuits 4:124. Medline

Kubin L, Alheid GF, Zuperku EJ, McCrimmon DR (2006) Central pathways of pulmonary and lower airway vagal afferents. J Appl Physiol 101:618–627. CrossRef Medline

Kuna ST (1986) Inhibition of inspiratory upper airway motoneuron activity by phasic volume feedback. J Appl Physiol 60:1373–1379. Medline

Li WC (2011) Generation of locomotion rhythms without inhibition in vertebrates: the search for pacemaker neurons. Integr Comp Biol 51:879–889. CrossRef Medline

Lumsden T (1923) Observation on the respiratory centres in the cat. J Physiol 57:153–160. Medline

Macdonald RL, Olsen RW (1994) GABA$_A$ receptor channels. Annu Rev Neurosci 17:569–602. CrossRef Medline

Manabe M, Ezure K (1988) Decrementing expiratory neurons of the Bötzinger complex. I. Response to lung inflation and axonal projection. Exp Brain Res 72:150–158. CrossRef Medline

Mellen NM, Roham M, Feldman JL (2004) Afferent modulation of neonatal rat respiratory rhythm in vitro: cellular and synaptic mechanisms. J Physiol 556:859–874. CrossRef Medline

Merrill EG (1981) Where are the real respiratory neurons? Fed Proc 40:2389–2394. Medline

Molkov YI, Abdala AP, Bacak BJ, Smith JC, Paton JF, Rybak IA (2010) Late-expiratory activity: emergence and interactions with the respiratory CPG. J Neurophysiol 104:2713–2729. CrossRef Medline

Pagliardini S, Janczewski WA, Tan W, Dickson CT, Deisseroth K, Feldman JL (2011) Active expiration induced by excitation of ventral medulla in adult anesthetized rats. J Neurosci 31:2895–2905. CrossRef Medline

Paxinos G, Carrive P, Wang H, Wang P, eds (1999) Chemoarchitectonic atlas of the rat brainstem. San Diego: Academic.

Pierrefiche O, Schwarzacher SW, Bischoff AM, Richter DW (1998) Blockade of synaptic inhibition within the pre-Bötzinger complex in the cat suppresses respiratory rhythm generation in vivo. J Physiol 509:245–254. CrossRef Medline

Richter DW (1982) Generation and maintenance of the respiratory rhythm. J Exp Biol 100:93–107. Medline

Richter DW, Ballanyi K, Schwarzacher S (1992) Mechanisms of respiratory rhythm generation. Curr Opin Neurobiol 2:788–793. CrossRef Medline

Rubin JE, Hayes JA, Mendenhall JL, Del Negro CA (2009) Calcium-activated nonspecific cation current and synaptic depression promote network-dependent burst oscillations. Proc Natl Acad Sci U S A 106:2939–2944. CrossRef Medline

Rubio JE (1972) A new mathematical model of the respiratory center. Bull Math Biophys 34:467–481. CrossRef Medline

Schmid K, Foutz AS, Denavit-SaubiéM (1996) Inhibitions mediated by glycine and GABAA receptors shape the discharge pattern of bulbar respiratory neurons. Brain Res 710:150–160. CrossRef Medline

Shao XM, Feldman JL (1997) Respiratory rhythm generation and synaptic inhibition of expiratory neurons in pre-Bötzinger complex: differential roles of glycinergic and GABAergic neural transmission. J Neurophysiol 77:1853–1860. Medline

Smith JC, Ellenberger HH, Ballanyi K, Richter DW, Feldman JL (1991) Pre-Bötzinger complex: a brainstem region that may generate respiratory rhythm in mammals. Science 254:726–729. CrossRef Medline

Smith JC, Abdala AP, Koizumi H, Rybak IA, Paton JF (2007) Spatial and functional architecture of the mammalian brain stem respiratory network: a hierarchy of three oscillatory mechanisms. J Neurophysiol 98:3370–3387. CrossRef Medline

Smith JC, Abdala AP, Borgmann A, Rybak IA, Paton JF (2012) Brainstem respiratory networks: building blocks and microcircuits. Trends Neurosci. Advance online publication. Retrieved January 30, 2013. doi: 10.1016/j.tins.2012.11.004. CrossRef Medline

St-John WM, Stornetta RL, Guyenet PG, Paton JF (2009) Location and properties of respiratory neurones with putative intrinsic bursting properties in the rat in situ. J Physiol 587:3175–3188. CrossRef Medline

Tan W, Janczewski WA, Yang P, Shao XM, Callaway EM, Feldman JL (2008) Silencing preBötzinger complex somatostatin-expressing neurons induces persistent apnea in awake rat. Nat Neurosci 11:538–540. CrossRef Medline

Tan W, Pagliardini S, Yang P, Janczewski WA, Feldman JL (2010) Projections of preBötzinger complex neurons in adult rats. J Comp Neurol 518:1862–1878. CrossRef Medline

Tan W, Sherman D, Turesson J, Shao XM, Janczewski WA, Feldman JL (2012) Reelin demarcates a subset of pre-Bötzinger complex neurons in adult rat. J Comp Neurol 520:606–619. CrossRef Medline

von Euler C (1983) On the central pattern generator for the basic breathing rhythmicity. J Appl Physiol 55:1647–1659. Medline

Winter SM, Fresemann J, Schnell C, Oku Y, Hirrlinger J, Hülsmann S (2009) Glycinergic interneurons are functionally integrated into the inspiratory network of mouse medullary slices. Pflugers Arch 458:459–469. CrossRef Medline

Younes MK, Remmers JE, Baker J (1978) Characteristics of inspiratory inhibition by phasic volume feedback in cats. J Appl Physiol 45: 80–86. Medline